



# A simple prediction model using size measures for discrimination of invasive adenocarcinomas among incidental pulmonary subsolid nodules considered for resection

Hyungjin Kim<sup>1</sup> · Jin Mo Goo<sup>1,2</sup> · Chang Min Park<sup>1,2</sup> 

Received: 21 March 2018 / Revised: 25 July 2018 / Accepted: 28 August 2018 / Published online: 25 September 2018  
© European Society of Radiology 2018

## Abstract

**Objectives** To develop and validate a concise prediction model using simple size measures for the discrimination of invasive pulmonary adenocarcinomas (IPAs) among incidentally detected subsolid nodules (SSNs) considered for resection and to compare its diagnostic performance with the Brock model.

**Methods** This retrospective institutional review board-approved study included 427 surgically resected SSNs (121 preinvasive lesions/minimally invasive adenocarcinomas [MIAs] and 306 IPAs) from 407 patients. After stratified random splitting of the study population into the training and validation sets (3:1), a simple logistic model was constructed using nodule size, solid proportion, and type for the differentiation of IPAs. Diagnostic performance of this model was compared with the original and modified Brock models using the DeLong method for area under the receiver-operating characteristic curve (AUC) and McNemar test for diagnostic sensitivity and specificity.

**Results** Our proposed model had an AUC of 0.859 in the validation set, while the original Brock model showed an AUC of 0.775 ( $p = 0.035$ ) and the modified Brock model exhibited an AUC of 0.787 ( $p = 0.006$ ). At equally high specificity of 90%, our proposed model exhibited significantly higher sensitivity (65.8%) than the original and modified Brock models (38.2% and 50.0%;  $p < 0.001$  and 0.008, respectively).

**Conclusions** Our study results demonstrated that the proposed concise model outperformed both Brock models, demonstrating its potential to be utilized as a specific tool to differentiate IPAs from preinvasive lesions and MIAs, which were considered for resection. External validation studies are warranted for the population with incidentally detected SSNs including small SSNs to confirm our observations.

## Key Points

- Size measures provided sufficient information for the risk stratification of surgical candidate incidental subsolid nodules.
- Our proposed concise model showed higher diagnostic performance than the Brock model for incidentally detected subsolid nodules.
- Our proposed model can specifically differentiate invasive adenocarcinomas among incidentally detected subsolid nodules and reduce overtreatment for indolent subsolid nodules.

**Keywords** Non-small-cell lung carcinoma · Adenocarcinoma · Multidetector computed tomography · Logistic models · Differential diagnosis

---

**Electronic supplementary material** The online version of this article (<https://doi.org/10.1007/s00330-018-5739-x>) contains supplementary material, which is available to authorized users.

---

✉ Chang Min Park  
cmpark.morphius@gmail.com

<sup>2</sup> Cancer Research Institute, Seoul National University, 101, Daehak-ro, Jongno-gu, Seoul 03080, Korea

<sup>1</sup> Department of Radiology, Seoul National University College of Medicine, and Institute of Radiation Medicine, Seoul National University Medical Research Center, 101, Daehak-ro, Jongno-gu, Seoul 03080, Korea

## Abbreviations

AAH	Atypical adenomatous hyperplasia
AIS	Adenocarcinoma-in-situ
AUC	Area under the receiver-operating characteristic curve
BTS	British Thoracic Society
IPA	Invasive pulmonary adenocarcinoma
MIA	Minimally invasive adenocarcinoma
NPV	Negative predictive value
PPV	Positive predictive value
PSN	Part-solid nodule
ROC	Receiver-operating characteristic
SSN	Subsolid nodule

## Introduction

In the management of persistent subsolid nodules (SSNs), differentiation of invasive pulmonary adenocarcinomas (IPAs) from preinvasive lesions and minimally invasive adenocarcinomas (MIAs) are of great clinical significance for the following reasons. First, preinvasive lesions and MIAs are candidates for sublobar resection whereas IPAs are not [1, 2]. Second, the necessity of immediate surgical resection may be obviated in cases of preinvasive lesions and MIAs, which can remain stable over several years [3, 4]. In addition, although sublobar resection may have less morbidity compared with lobectomy, previous studies have shown that perioperative morbidity was not negligible (7–19%) [5, 6]. Therefore, in this context, CT surveillance for potentially indolent lesions may be a more reasonable approach.

At present, the British Thoracic Society (BTS) suggests risk calculations using the Brock model, a relatively complex tool that requires nine inputs, for the management of both screening- and incidentally detected SSNs [7] even though it is at odds with the actual clinical context in certain situations. Specifically, differentiation of adenocarcinoma in situ (AIS), which is considered a malignancy in the Brock model [8], may not be of much interest to clinicians and radiologists, as AIS does not require immediate therapeutic intervention. Furthermore, the reported proportion of IPAs among persistent, incidental SSNs has been shown to be significantly higher than the 2.9% reported with the original Brock model [8–11]. Therefore, the diagnostic performance of the Brock model may be limited in the setting of incidentally detected persistent SSNs, leaving an unmet need for a prediction model that can specifically discriminate IPAs among incidental SSNs.

One of the key elements for the evaluation of SSNs is solid portion size [12]. Several studies have revealed that the solid portions in part-solid nodules (PSNs) are well correlated with the pathologic invasive adenocarcinoma component [10, 13, 14]. However, the Brock model does not incorporate solid portion size as an input variable; thus, the BTS recommends

that the solid component be considered to refine the estimate of malignancy [7]. Nevertheless, until now, there have been no concrete suggestions or recommended cutoff points for the assessment of the solid component of PSNs [7].

In this study, we hypothesized that a concise prediction model using only size measures such as nodule size and solid portion size would be a sufficient alternative to the Brock model for the risk stratification of incidental SSNs, particularly in terms of discriminating IPAs from other potential surgical candidates. Thus, we aimed to develop and validate a concise model using size measures to specifically differentiate IPAs from other incidental SSNs and to compare its diagnostic performance with the original and modified Brock models.

## Methods

This retrospective observational study was approved by the Institutional Review Board of Seoul National University Hospital, and the requirement for written informed consent was waived.

### Study participants

Patients who underwent surgical resections for lung cancer at a tertiary referral hospital between 2011 and 2015 were retrospectively identified. Among 1915 lung cancer patients, 522 had SSNs of the adenocarcinoma spectrum including atypical adenomatous hyperplasia (AAH), AIS, MIA, and IPA. Among them, 76 patients with nodules < 5 mm or > 3 cm and 39 patients whose family history of lung cancer (one of the input variables of the Brock model) were not available were excluded. Consequently, 407 patients finally comprised our study population. Among these patients, 18 had 2 nodules and 1 patient had 3 nodules. Therefore, a total of 427 nodules from 407 patients were analyzed in the present study (Table 1). There were 18 AAHs, 50 AIS, 53 MIAs, and 306 IPAs.

Part of the study population was reported in past studies [15–19]. However, none of those studies focused on the comparison of diagnostic performances between the prediction models, and the topics were completely different from that of the present study.

### Data collection

Clinical variables (sex, age, and family history of lung cancer) and pathologic diagnoses were collected from the electronic medical records. Nodule characteristics (nodule size, solid portion size, location, type [pure ground glass vs. part solid], spiculation, and nodule count per scan) and the presence of emphysema were evaluated on preoperative thin-section chest CT scans by three radiologists (J.P., W.H.L., and H.K.) who

**Table 1** Demographic and clinico-radiologic characteristics of subsolid nodules

Variable	Subcategory	Preinvasive lesion and MIA ( <i>n</i> = 121)	Invasive adenocarcinoma ( <i>n</i> = 306)	Total ( <i>n</i> = 427)	<i>p</i> value <sup>b</sup>
Sex	Male	50 (41.3)	133 (43.5)	183 (42.8)	0.687
	Female	71 (58.7)	173 (56.5)	244 (57.1)	
Age (years) <sup>a</sup>		58 (52, 66)	63 (56, 70)	61 (54, 69)	< 0.001
Nodule size (mm) <sup>a</sup>		11.9 (9.2, 15.4)	17.4 (13.2, 22.2)	15.7 (11.7, 20.9)	< 0.001
Solid portion size (mm) <sup>a</sup>		0 (0, 4.0)	7.9 (4.1, 13.6)	5.4 (1.9, 11.1)	< 0.001
Solid proportion (%) <sup>a</sup>		0 (0, 29.7)	50.4 (27.9, 65.1)	38.7 (13.3, 61.2)	< 0.001
Nodule type	Pure ground glass	69 (57.0)	37 (12.1)	106 (24.8)	< 0.001
	Part solid	52 (43.0)	269 (87.9)	321 (75.2)	
Location	Upper lobe	70 (57.9)	189 (61.8)	259 (60.7)	0.456
	Other lobes	51 (42.1)	117 (38.2)	168 (39.3)	
Family history of lung cancer	Yes	3 (2.5)	13 (4.2)	16 (3.7)	0.573
	No	118 (97.5)	293 (95.8)	411 (96.3)	
Emphysema	Yes	13 (10.7)	31 (10.1)	44 (10.3)	0.851
	No	108 (89.3)	275 (89.9)	383 (89.7)	
Nodule count per scan <sup>a</sup>		3 (1, 6)	3 (1, 5)	3 (1, 5)	0.528
Spiculation	Yes	13 (10.7)	125 (40.8)	138 (32.3)	< 0.001
	No	108 (89.3)	181 (59.2)	289 (67.7)	

Unless otherwise specified, data are numbers of patients (with percentages in parentheses)

<sup>a</sup>Data are median (with interquartile range in parentheses) *MIA* minimally invasive adenocarcinoma

<sup>b</sup>Clinico-radiologic variables were compared between preinvasive lesions/MIAs and invasive adenocarcinomas using the Mann-Whitney *U* test for continuous variables and the chi-square test or Fisher's exact test for categorical variables

were blinded to the pathologic diagnosis. Each nodule was then analyzed once by one of the radiologists. Median interval between CT scan and surgery was 6 days (interquartile range, 1–25 days).

Longest diameter of the nodule and its solid portion (in cases of PSNs) were measured on the lung window setting of CT scans using an electronic caliper at a picture archiving and communication system. The solid proportion was then calculated by dividing the solid portion size by the nodule size. Nodule type was also determined on the lung window setting according to the definition established by the Fleischner society [20, 21].

### Pathologic diagnosis

Pathologic diagnoses were used as the reference standard and were determined by the attending pathologists of our hospital as part of the routine clinical process according to the 2011 lung adenocarcinoma classification described by the International Association for the Study of Lung Cancer/American Thoracic Society/European Respiratory Society [22]. That is, the pathologic specimens of the study population were not reviewed again particularly for this study. In our institution, 10% buffered formalin was infused to inflate and fix all surgical specimens containing SSNs via the transpleural

and transbronchial approach to precisely measure the invasive adenocarcinoma component [10].

### Statistical analysis

Clinico-radiologic variables were compared between preinvasive lesions/MIAs and IPAs using the Mann-Whitney *U* test for continuous variables and the chi-square test or Fisher's exact test for categorical variables.

Thereafter, the study population was partitioned into a training set (321 nodules; 91 preinvasive lesions/MIAs and 230 IPAs) and a validation set (106 nodules; 30 preinvasive lesions/MIAs and 76 IPAs) using stratified random sampling (see also [Electronic Supplementary Material](#) for the 1000-times repeated random splitting and its results). The original Brock model published by McWilliams et al [8] was initially tested for both data sets, and the model-predicted probability for IPAs was recorded. Then, the beta coefficients of the logistic regression model were adjusted to our study population (hence, the modified Brock model) by fitting the model to our training set. This approach was adopted to guarantee a fair comparison between the Brock model and our proposed model. This modified Brock model was validated using the validation set, which was unseen data to test the model's performance. Finally, the proposed model was developed using

logistic regression analysis with input variables of nodule size, solid proportion, and nodule type. Solid proportion was used instead of solid portion size as the solid portion size had a linear relationship with nodule size. Variable selection was not conducted, and the enter method was used as these features were demonstrated to have a substantial association with the invasiveness of SSNs [18, 21]. All values were not pre-processed. This concise prediction model was trained using the training set and validated using the validation set. After acquisition of the predicted probability for IPAs of these three models, receiver-operating characteristic (ROC) curve analysis was performed, and the area under the ROC curve (AUC) of each prediction model was calculated. The AUC of the proposed model was then compared with the original and modified Brock models using the method described by DeLong et al [23].

Model performance was also assessed in terms of diagnostic sensitivity, specificity, accuracy, positive predictive value (PPV), and negative predictive value (NPV). For comparison, cutoff values that provide a high sensitivity (89.5%) and high specificity (90%), respectively, were determined for each model. Thereafter, specificity was compared between the models using the McNemar test in the setting of equally high sensitivity (89.5%) and sensitivity in the setting of equally high specificity (90%). Additionally, to investigate the varying

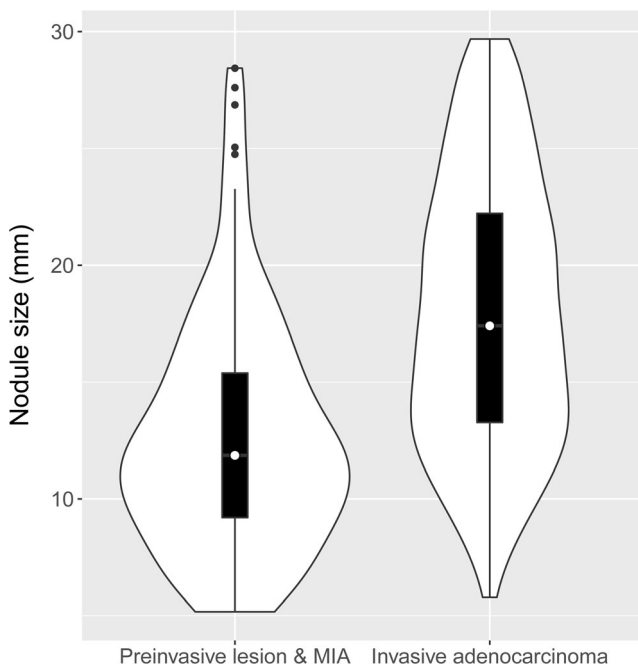


**Fig. 1** Distribution of nodule size. Violin plots describe the distribution of nodule size in terms of kernel density estimation according to size with internal box plots. Median size of the preinvasive lesions and MIAs (median, 11.9 mm; interquartile range, 9.2–15.4 mm) was smaller than that of invasive adenocarcinomas (median, 17.4 mm; interquartile range, 13.2–22.2 mm). However, discrimination solely based on nodule size was not feasible given the wide range of sizes in both diagnostic categories. MIA, minimally invasive adenocarcinoma

diagnostic sensitivities and specificities depending on the cut-off values, empirical cutoff points of 0.7 and 0.8 were applied to the models, and performance measures were calculated.

Model calibration was evaluated using the Hosmer-Lemeshow test for the ten probability groups (deciles). Finally, decision-curve analysis was performed to quantify and compare the clinical usefulness of the models [24, 25].

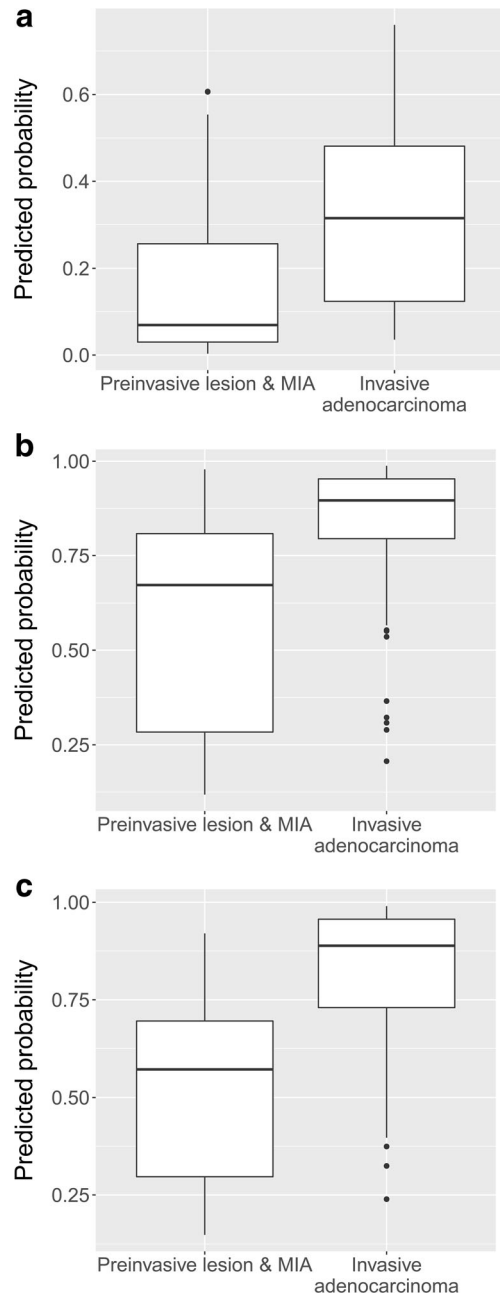


**Fig. 2** Distribution of probabilities for subsolid nodules. There was considerable overlap in the predicted probabilities between preinvasive lesions/minimally invasive adenocarcinomas and invasive adenocarcinomas for the original Brock model (a). The extent of overlap decreased for the modified Brock model (b) and the proposed model (c)

Decision-curve analysis is a simple approach that calculates the net benefits (NBs) across a range of thresholds. NB is determined as follows:

$$NB = \frac{\text{True positive} - w \times \text{False positive}}{\text{Total number of patients}}$$

where  $w$  is the weight equal to the odds of the cutoff [24, 25].

All above-mentioned analyses were conducted on a per nodule basis and within patient correlation or the clustering effect was not considered given the fact that each nodule among multiple SSNs was considered an independent event [26]. All statistical analyses were performed using a commercial software program (MedCalc version 12.3.0, MedCalc Software) and R software, version 3.1.0 (<http://www.R-project.org>; package: caret, ROCR, and PredictABEL).  $P < 0.05$  was considered to indicate statistical significance and, as stated previously, patients with missing variables were excluded from analysis and their data were not imputed.

## Results

### Comparison of variables between preinvasive lesions/MIAs and IPAs

There were 121 preinvasive lesions/MIAs and 306 IPAs. Patients with IPAs were significantly older (median, 63 years) than those with preinvasive lesions/MIAs (median, 58 years;  $p < 0.001$ ). IPAs were significantly larger in terms of whole nodule size (median, 17.4 vs. 11.9 mm;  $p < 0.001$ ; Fig. 1) and solid portion size (median, 7.9 vs. 0 mm;  $p < 0.001$ ) than

preinvasive lesions/MIAs. In addition, IPAs were more spiculated (40.8% vs. 10.7%;  $p < 0.001$ ) and were more likely to be part solid (87.9% vs. 43.0%;  $p < 0.001$ ). There were no significant differences in sex, lesion location, family history of lung cancer, presence of emphysema, and nodule count per scan (all  $p > 0.05$ ; Table 1).

### Diagnostic performance of the prediction models

There was considerable overlap in the model-predicted probabilities between preinvasive lesions/MIAs and IPAs for the original Brock model (Fig. 2a). The extent of overlap of the probabilities was smaller in the modified Brock model (Fig. 2b) and the proposed model (Fig. 2c).

To assess diagnostic performance, the original Brock model was applied to the training set as well as to the validation set. AUCs were 0.795 and 0.775, respectively. The modified Brock model, of which the regression coefficients were adjusted and fitted to the current study population of incidental SSNs (Table 2), exhibited an AUC of 0.844 in the training set. However, the AUC of the modified Brock model dropped to 0.787 in the validation set, which was indicative of overfitting. Our proposed model (Table 2) had AUCs of 0.843 in the training set and 0.859 in the validation set. This simple model showed significantly higher diagnostic performance than the original or modified Brock models ( $p = 0.035$  and  $0.006$ , respectively; Table 3; see ROC curves in Fig. 3) for the validation set.

At equally high sensitivity (89.5%), the original Brock model provided a specificity, accuracy, PPV, and NPV of 53.3%, 79.2%, 82.9%, and 66.7%, respectively. The modified Brock model exhibited a specificity, accuracy, PPV, and NPV of 43.3%, 76.4%, 80.0%, and 61.9%, respectively. In

**Table 2** Modified Brock model and the proposed model for risk prediction of pulmonary subsolid nodules

Variable	Modified Brock model			Proposed model		
	Odds ratio (95% CI)	<i>p</i> value	Beta coefficient	Odds ratio (95% CI)	<i>p</i> value	Beta coefficient
Sex: female vs. male	0.57 (0.30, 1.09)	0.094	-0.5538	-	-	-
Age: per year	1.01 (0.98, 1.05)	0.398	0.0140	-	-	-
Upper lobe: yes vs. no	1.02 (0.55, 1.88)	0.951	0.0194	-	-	-
Family history of lung cancer: yes vs. no	1.53 (0.30, 10.34)	0.6311	0.4276	-	-	-
Emphysema: yes vs. no	0.69 (0.25, 1.98)	0.475	-0.3773	-	-	-
Nodule count per scan, per each additional nodule	0.97 (0.91, 1.03)	0.253	-0.0356	-	-	-
Spiculation: yes or no	3.52 (1.50, 9.39)	0.006	1.2588	-	-	-
Nodule size	1.13 (1.07, 1.21)	< 0.001	0.1250	1.16 (1.09, 1.24)	< 0.001	0.1475
Nodule type: part solid vs. pure ground glass	5.60 (2.96, 10.83)	< 0.001	1.7224	1.69 (0.61, 4.69)	0.311	0.5248
Solid proportion per percentage	-	-	-	1.03 (1.01, 1.05)	0.003	0.0303
Model constant			-2.7071			-2.5745

CI confidence interval

**Table 3** Performance of the three prediction models for discrimination of invasive pulmonary adenocarcinomas

Model	Training set			Validation set		
	AUC	95% CI	<i>p</i> value <sup>a</sup>	AUC	95% CI	<i>p</i> value <sup>a</sup>
Original Brock model	0.795	0.747, 0.838	0.019	0.775	0.669, 0.882	0.035
Modified Brock model	0.844	0.800, 0.882	0.944	0.787	0.697, 0.861	0.006
Proposed model	0.843	0.798, 0.881		0.859	0.778, 0.919	

AUC area under the receiver-operating characteristic curve, CI confidence interval

<sup>a</sup> AUC of the proposed model was compared to those of the Brock models using the DeLong method [23]

comparison, the proposed model showed a specificity, accuracy, PPV, and NPV of 50.0%, 78.3%, 81.9%, and 65.2%, respectively. No significant differences in specificity between the proposed and Brock models were observed ( $p = 1.000$  and  $0.500$ ).

At equally high specificity (90%), the proposed model exhibited significantly higher sensitivity (65.8%) than the original and modified Brock models (38.2% and 50.0%;  $p < 0.001$  and  $0.008$ , respectively). Diagnostic accuracies, PPVs, and NPVs were 52.8%, 90.6%, and 36.5% for the original Brock model and 61.3%, 92.7%, and 41.5% for the modified Brock model, respectively. Diagnostic accuracy, PPV, and NPV were 72.6%, 94.3%, and 50.9% for the proposed model, respectively. Prevalence of IPA was 71.7% (76/106) in the validation set.

At an empirical cutoff of 0.7, the proposed model demonstrated a sensitivity, specificity, accuracy, PPV, and NPV of 81.6%, 76.7%, 80.2%, 89.9%, and 62.2%, respectively. The diagnostic sensitivity and specificity of the

models varying according to the cutoff values are shown in Table 4.

**Model calibration**

The original Brock model showed poor calibration ( $p < 0.001$ ; Fig. 4a), whereas the modified Brock model ( $p = 0.149$ ; Fig. 4b) and proposed model demonstrated adequate calibration ( $p = 0.552$ ; Fig. 4c).

**Decision curve analysis**

Across a range of cutoff values, the proposed model exhibited the largest NBs as shown in Fig. 5. At a cutoff of 0.7, NBs were 43.1% for the proposed model, 28.6% for the modified Brock model, and 2.8% for the original Brock model. At a cutoff of 0.8, NBs were 34.9% for the proposed model, 22.6% for the modified Brock model, and 0% for the original Brock model.

**Fig. 3** Receiver-operating characteristic curves for the discrimination of IPAs. The simple proposed model showed higher discriminative performance (AUC, 0.859) than the original (AUC, 0.775) and modified Brock models (AUC, 0.787). AUC, area under the curve; IPA, invasive pulmonary adenocarcinoma

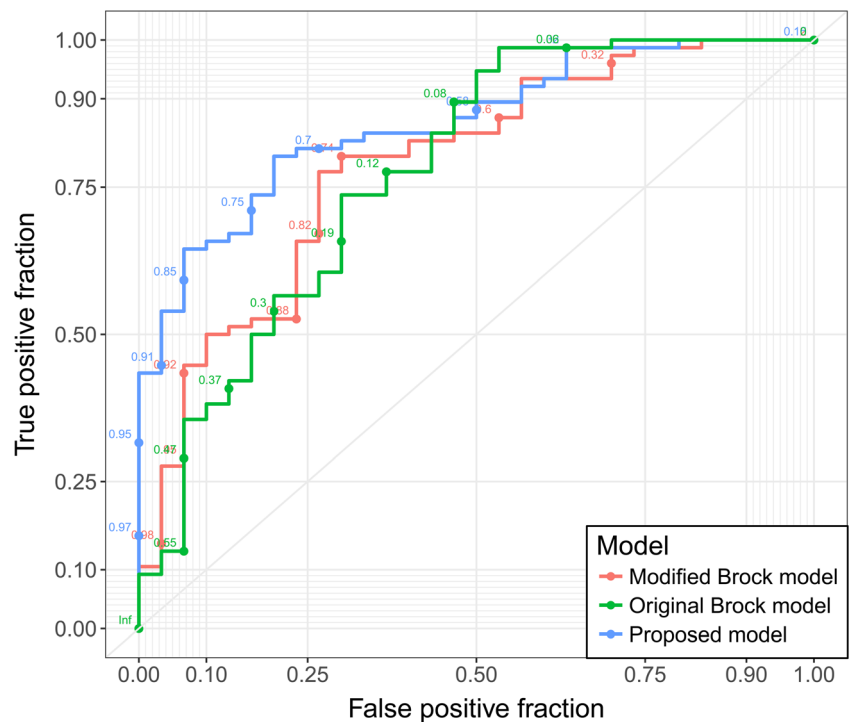


**Table 4** Performance measures of the three prediction models according to cutoff values

Model	Cutoff	Sensitivity	Specificity	Accuracy	PPV	NPV
Original Brock model	0.1 <sup>a</sup>	81.6	56.7	74.5	82.7	54.8
	0.7	3.9	100	31.1	100	29.1
	0.8	0	100	28.3	N/A	28.3
Modified Brock model	0.1 <sup>a</sup>	100	0	71.7	71.7	N/A
	0.7	82.9	53.3	74.5	81.8	55.2
	0.8	73.7	73.3	73.6	87.5	52.4
Proposed model	0.1 <sup>a</sup>	100	0	71.7	71.7	N/A
	0.7	81.6	76.7	80.2	89.9	62.2
	0.8	64.5	90.0	71.7	94.2	50.0

Performance measures are in percentages

NPV negative predictive value, PPV positive predictive value

<sup>a</sup> A cutoff of 10% predicted probability was used as suggested by the British Thoracic Society for the original Brock model [7]

## Discussion

Our study demonstrated that the newly proposed model using simple size measures showed higher diagnostic performance for the discrimination of IPAs among incidentally detected SSNs that were recommended to be resected than the original or modified Brock models, providing higher

sensitivity (65.8% vs. 38.2%–50%) at the same specificity of 90%.

Considering that the PPV of our proposed model was 94.3%, this model developed to differentiate IPAs may be used to mitigate the overtreatment of SSNs considered to be surgical candidates. Indeed, overdiagnosis and overtreatment have long been issues in lung cancer screening studies [27]. A

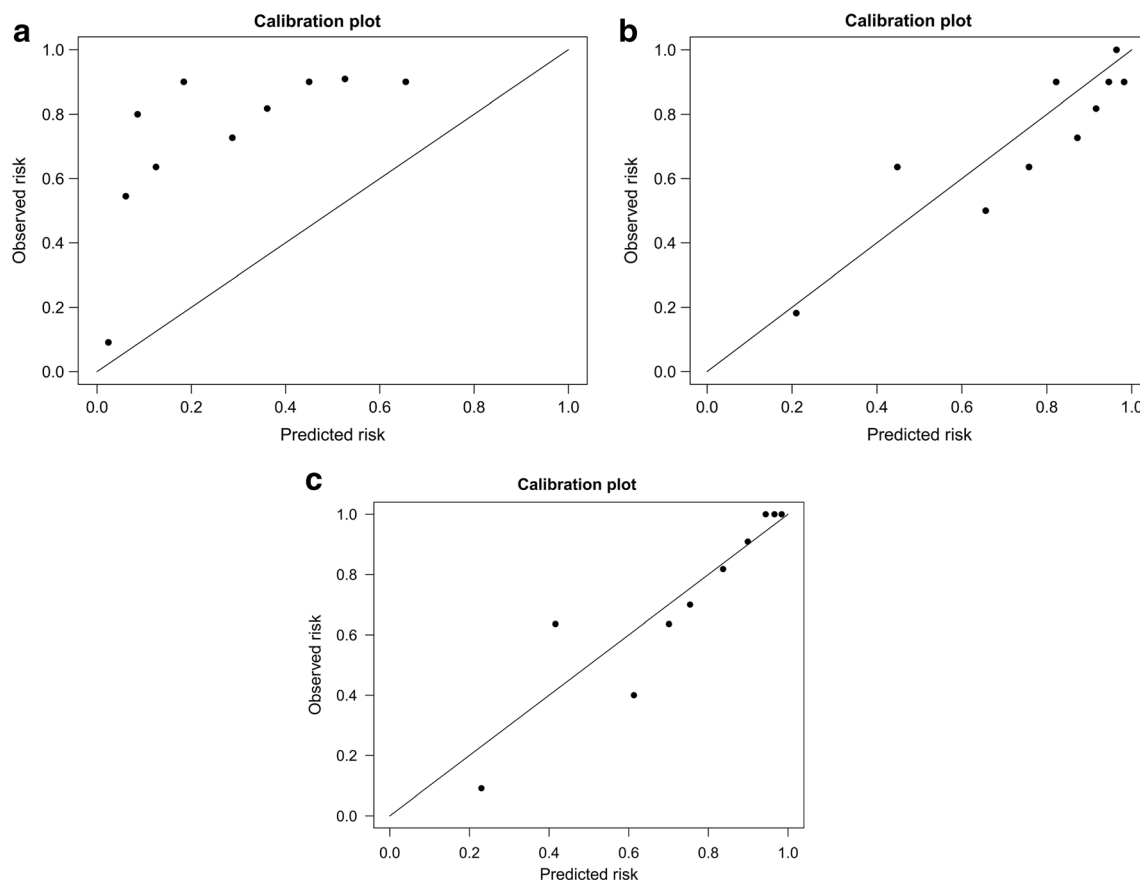


**Fig. 4** Calibration plots of the prediction models. The original Brock model showed poor calibration (a), while the modified Brock model (b) and the proposed model demonstrated adequate calibration (c)

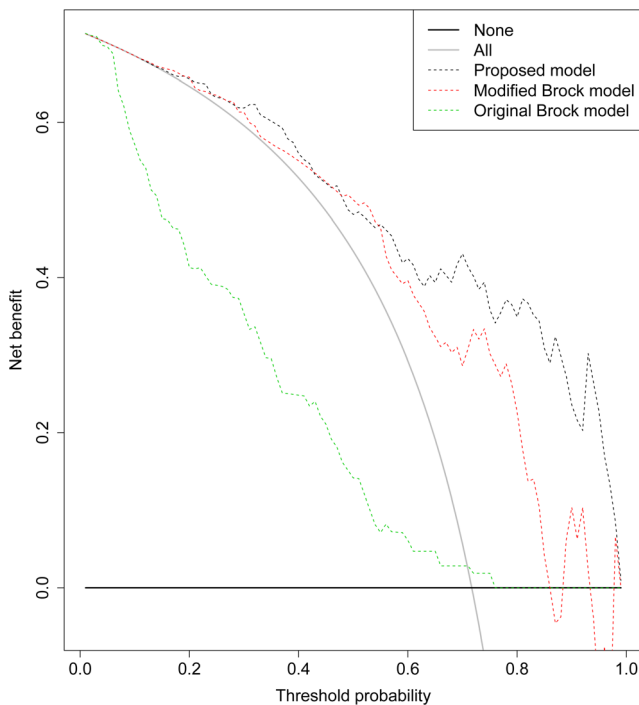


**Fig. 5** Decision curves for the predicted probabilities in the validation data set. The proposed model exhibited higher net benefits compared with the original and modified Brock models for cutoffs  $\geq 0.55$ . This implies that additional true positives can be identified without increasing the false-positive rate using the proposed model

substantial portion of screening-detected lung cancers were shown to be indolent with 20–25% of cancers detected estimated to be overdiagnosed [27]. We believe that these issues would have equivalent importance for incidental SSNs, a subset of which may not show invasive growth over years of follow-up [28] with no reported difference in prognosis even after observation [4]. Therefore, treatment for indolent SSNs should be determined on the basis of a comprehensive evaluation of life expectancy, patient apprehension, and the likelihood of malignancy. One concern regarding the newly proposed model, however, may be its low NPV (50.9%). Yet, although some IPAs might be missed at initial risk calculation, follow-up for SSNs with solid portions  $\geq 6$  mm at 3–6-month intervals would be able to safely identify IPAs that should be excised [3]. Increases in nodule size, solid portion size, or attenuation, which are indicators of IPAs for SSNs, can be monitored at follow-up CT scans [12].

The Brock model incorporates various clinico-radiologic variables of which the full model includes nine features. As analyzed in our study, statistical significance was not observed for nodule location, family history of lung cancer, emphysema, and nodule count per scan between preinvasive lesions/MIAs and IPAs. This lack of statistical power may be partly due to the number of the study population. However, variables such as emphysema and nodule count have little biologic and epidemiologic background for SSNs as explanatory variables.

In addition, although some controversy remains, Smith et al [29] reported that no significant association between lung adenocarcinoma and emphysema was observed (adjusted odds ratio, 1.0) when other histologies were censored from the analysis.

The usage of a concise prediction model with fewer variables as in our proposed model provides benefits in terms of practicality as missing clinical information in routine practice often limits the application of the patient data to a model requiring multiple variables. In addition, complicated models may be subject to multiple sources of variation during data acquisition as well as overfitting when applied to an independent data set [24].

In clinical practice, the diagnosis or management of SSNs is determined by measuring solid portion size. When the nodules were classified into the two groups based on the solid portion size cutoff of 5 mm, diagnostic performances for IPAs were as follows: sensitivity, 72.5%; specificity, 81.0%; accuracy, 74.9%; PPV, 90.6%; NPV, 53.8%. The low specificity implied that this criterion alone was suboptimal. In addition, it could not be applied to the pure ground-glass nodules, which do not have any solid portions.

There were several limitations to this study that need to be mentioned. First, our study was performed retrospectively and included patients who underwent surgical resections. Therefore, our study may not be free from selection bias. However, analysis of the resected nodules was inevitable given the indolent nature of SSNs and the fact that even nodules with invasive components may remain unchanged over years of CT surveillance. Thus, histology (reference standard) could not be determined based on follow-up studies. Nevertheless, we admit that our proposed model may not be directly applied to screening-detected SSNs or small indolent SSNs, which are not regarded as targets of surgical resections. Further investigation of screening-detected SSNs or small indolent SSNs is warranted to evaluate the performance of our model in each clinical setting. Second, our study sample size was not calculated prior to the investigation. Nevertheless, a large retrospective cohort could be analyzed in this study. Third, radiologic nodule information was extracted from a heterogeneous CT data set, in which CT acquisition parameters such as radiation dosage, slice thickness, or contrast-enhancement were not uniform across the study population. However, we can assume that these factors might have had little effect on the size measurements. Indeed, all CT scans had thin-section images (slice thickness  $\leq 1.5$  mm), which guaranteed the adequate evaluation of the ground-glass and solid components of SSNs.

In conclusion, we here propose a simple risk prediction model using three input variables of nodule size, solid proportion, and nodule type, which can be easily obtained from CT imaging. Our results demonstrated that our proposed model may be utilized as a specific tool to discriminate IPAs from preinvasive lesions and MIAs, which can be followed up with

CT scans instead of immediate surgical intervention. Our model can also be used as a more practical tool with fewer variables than the Brock model. Further external validation of our findings is required in a larger prospective study including smaller SSNs.

**Acknowledgements** We express our gratitude to Sunkyung Jeon, Jong Hyuk Lee, Su Yeon Ahn, Roh-Eul Yoo, Hyun-ju Lim, Juil Park, and Woo Hyeon Lim for data acquisition. We also thank Chris Woo for the manuscript editing.

**Funding** This study was supported by Basic Science Research Program through the National Research Foundation of Korea (NRF), funded by the Ministry of Science, ICT & Future Planning (grant no. 2017R1A2B4008517).

## Compliance with ethical standards

**Guarantor** The scientific guarantor of this publication is Chang Min Park.

**Conflict of interest** The authors of this manuscript declare no relationships with any companies, whose products or services may be related to the subject matter of the article.

**Statistics and biometry** No complex statistical methods were necessary for this paper.

**Informed consent** Written informed consent was waived by the Institutional Review Board.

**Ethical approval** Institutional Review Board approval was obtained.

**Study subjects or cohorts overlap** Some study subjects or cohorts have been previously reported in journal articles (Eur Radiol 2016 26:4465–4474; Eur J Radiol 2016 85:1174–1180; Eur Radiol 2017 27:3266–3274; Eur Radiol 2017 10.1007/s00330-017-5171-7; Eur Radiol 2017 27:1369–1376).

## Methodology

- retrospective
- diagnostic or prognostic study
- performed at one institution

## References

1. Tsutani Y, Miyata Y, Nakayama H et al (2014) Appropriate sublobar resection choice for ground glass opacity-dominant clinical stage IA lung adenocarcinoma: wedge resection or segmentectomy. *Chest* 145:66–71
2. Jin C, Cao J, Cai Y et al (2017) A nomogram for predicting the risk of invasive pulmonary adenocarcinoma for patients with solitary peripheral subsolid nodules. *J Thorac Cardiovasc Surg* 153(462–469):e461
3. MacMahon H, Naidich DP, Goo JM et al (2017) Guidelines for management of incidental pulmonary nodules detected on CT images: from the Fleischner Society 2017. *Radiology* 284:228–243
4. Lee JH, Park CM, Kim H, Hwang EJ, Park J, Goo JM (2017) Persistent part-solid nodules with solid part of 5 mm or smaller: can the 'follow-up and surgical resection after interval growth' policy have a negative effect on patient prognosis? *Eur Radiol* 27: 195–202
5. Billmeier SE, Ayanian JZ, Zaslavsky AM, Nerenz DR, Jaklitsch MT, Rogers SO (2011) Predictors and outcomes of limited resection for early-stage non-small cell lung cancer. *J Natl Cancer Inst* 103: 1621–1629
6. Kim D, Ferraris VA, Davenport D, Saha S (2015) Outcomes of lobar and sublobar resections for non-small-cell lung cancer: a single-center experience. *South Med J* 108:230–234
7. Callister ME, Baldwin DR, Akram AR et al (2015) British Thoracic Society guidelines for the investigation and management of pulmonary nodules. *Thorax* 70(Suppl 2):ii1–ii54
8. McWilliams A, Tammemagi MC, Mayo JR et al (2013) Probability of cancer in pulmonary nodules detected on first screening CT. *N Engl J Med* 369:910–919
9. Chae HD, Park CM, Park SJ, Lee SM, Kim KG, Goo JM (2014) Computerized texture analysis of persistent part-solid ground-glass nodules: differentiation of preinvasive lesions from invasive pulmonary adenocarcinomas. *Radiology* 273:285–293
10. Lee KH, Goo JM, Park SJ et al (2014) Correlation between the size of the solid component on thin-section CT and the invasive component on pathology in small lung adenocarcinomas manifesting as ground-glass nodules. *J Thorac Oncol* 9:74–82
11. Henschke CI, Yankelevitz DF, Mirtcheva R et al (2002) CT screening for lung cancer: frequency and significance of part-solid and nonsolid nodules. *AJR Am J Roentgenol* 178:1053–1057
12. Kim H, Park CM, Koh JM, Lee SM, Goo JM (2014) Pulmonary subsolid nodules: what radiologists need to know about the imaging features and management strategy. *Diagn Interv Radiol* 20:47–57
13. Ko JP, Suh J, Ibidapo O et al (2016) Lung adenocarcinoma: correlation of quantitative CT findings with pathologic findings. *Radiology* 280:931–939
14. Yanagawa M, Johkoh T, Noguchi M et al (2017) Radiological prediction of tumor invasiveness of lung adenocarcinoma on thin-section CT. *Medicine (Baltimore)* 96:e6331
15. Cohen JG, Goo JM, Yoo RE et al (2016) Software performance in segmenting ground-glass and solid components of subsolid nodules in pulmonary adenocarcinomas. *Eur Radiol* 26:4465–4474
16. Cohen JG, Goo JM, Yoo RE et al (2016) The effect of late-phase contrast enhancement on semi-automatic software measurements of CT attenuation and volume of part-solid nodules in lung adenocarcinomas. *Eur J Radiol* 85:1174–1180
17. Cohen JG, Kim H, Park SB et al (2017) Comparison of the effects of model-based iterative reconstruction and filtered back projection algorithms on software measurements in pulmonary subsolid nodules. *Eur Radiol* 27:3266–3274
18. Kim H, Park CM, Hwang EJ, Ahn SY, Goo JM (2018) Pulmonary subsolid nodules: value of semi-automatic measurement in diagnostic accuracy, diagnostic reproducibility and nodule classification agreement. *Eur Radiol* 28:2124–2133
19. Yoo RE, Goo JM, Hwang EJ et al (2017) Retrospective assessment of interobserver agreement and accuracy in classifications and measurements in subsolid nodules with solid components less than 8mm: which window setting is better? *Eur Radiol* 27:1369–1376
20. Hansell DM, Bankier AA, MacMahon H, McLoud TC, Müller NL, Remy J (2008) Fleischner Society: glossary of terms for thoracic imaging. *Radiology* 246:697–722
21. Naidich DP, Bankier AA, MacMahon H et al (2013) Recommendations for the management of subsolid pulmonary nodules detected at CT: a statement from the Fleischner Society. *Radiology* 266:304–317
22. Travis WD, Brambilla E, Noguchi M et al (2011) International Association for the Study of Lung Cancer/American Thoracic Society/European Respiratory Society international multidisciplinary classification of lung adenocarcinoma. *J Thorac Oncol* 6:244–285

23. DeLong ER, DeLong DM, Clarke-Pearson DL (1988) Comparing the areas under two or more correlated receiver operating characteristic curves: a nonparametric approach. *Biometrics* 44:837–845
24. Steyerberg EW, Vergouwe Y (2014) Towards better clinical prediction models: seven steps for development and an ABCD for validation. *Eur Heart J* 35:1925–1931
25. Steyerberg EW, Vickers AJ, Cook NR et al (2010) Assessing the performance of prediction models: a framework for traditional and novel measures. *Epidemiology* 21:128–138
26. Chung JH, Choe G, Jheon S et al (2009) Epidermal growth factor receptor mutation and pathologic-radiologic correlation between multiple lung nodules with ground-glass opacity differentiates multicentric origin from intrapulmonary spread. *J Thorac Oncol* 4:1490–1495
27. Esserman LJ, Thompson IM, Reid B et al (2014) Addressing overdiagnosis and overtreatment in cancer: a prescription for change. *Lancet Oncol* 15:e234–e242
28. Kakinuma R, Noguchi M, Ashizawa K et al (2016) Natural history of pulmonary subsolid nodules: a prospective multicenter study. *J Thorac Oncol* 11:1012–1028
29. Smith BM, Schwartzman K, Kovacina B et al (2012) Lung cancer histologies associated with emphysema on computed tomography. *Lung Cancer* 76:61–66